Polymer 54 (2013) 6886–6893

Contents lists available at ScienceDirect

Polymer

journal homepage: www.elsevier.com/locate/polymer

In-situ polymerization of styrene in AAO nanocavities

Juan M. Giussi [a,b,c], Iwona Blaszczyk-Lezak [a], M. Susana Cortizo [b,c], Carmen Mijangos [a,*]

[a] Instituto de Ciencia y Tecnología de Polímeros, CSIC, Juan de la Cierva 3, 28006 Madrid, Spain
[b] Instituto de Investigaciones Fisicoquímicas Teóricas y Aplicadas (INIFTA), Universidad Nacional de La Plata, CONICET, CC 16 Suc. 4, 1900 La Plata, Argentina
[c] Laboratorio de Estudio de Compuestos Orgánicos, Universidad Nacional de La Plata, 47 y 115, 1900 La Plata, Argentina

ARTICLE INFO

Article history:
Received 14 August 2013
Received in revised form
16 October 2013
Accepted 23 October 2013
Available online 30 October 2013

Keywords:
Nanofabrication
Nanoconfinement
Microstructure

ABSTRACT

One of the most promising aspects of the anodic aluminium oxide (AAO) template is the ability to generate a variety of different hierarchical one-dimensional (1D) polymer morphologies with structural definition on the nanometric scale. In-situ polymerization of monomers in reduced space of porous AAO template nanocavities can give rise to the direct production of versatile polymer nanostructures. In this work, porous AAO devices of 35 nm of diameter have been obtained by a two-step electrochemical anodization process and used as a nanoreactor to study the radical polymerization kinetics of styrene (St) in confinement and the results compared to those of polymerization in bulk. SEM morphological study has been conducted to establish the final structure of obtained polymer nanostructures. Confocal Raman microscopy has been performed to study the formation of the polymer through the AAO cavities as a function of time and with this methodology it has been possible to establish the monomer conversion for styrenic polymerization in AAO devices. Polystyrene obtained in the nanoreactor was characterized by SEC, NMR, TGA and DSC and the properties compared with those of bulk polymer. It was found that both the average molecular weights and polydispersity index of nanostructured polymer are lower than those obtained for bulk polymer. NMR studies have shown that the use of a reactor with nanometric size dimensions gave the obtained polystyrene greater stereospecificity than that obtained in bulk. Thermal stability and glass transition temperature (T_g) values are higher for nanostructured than bulk polymers. Moreover, the methodology proposed in this work, using AAO nanocavities as nanoreactors for polymerization reaction, can be generalized and applied to obtain polymer nanostructures of very different chemical nature and morphology by choosing the appropriate monomer or monomer reactants and by tailoring the dimension of AAO cylindrical nanocavities, that is, diameter from 20 to 400 nm and length from a few to hundreds of microns.

1. Introduction

One of the most promising aspects of the anodic aluminium oxide (AAO) template is the ability to generate a variety of different hierarchical one-dimensional (1D) polymer morphologies with structural definition on the nanometric scale. 1D nanostructures from PLLA, PMMA, PEO, PDMS, etc. and from polymer based composites have been obtained from AAO templates by polymer infiltration and replication methods and they have found potential applications as scaffolds for tissue engineering, miniaturized sensors, magnetic labels and others [1–8]. Moreover, the confining of the polymers to nanoscale has given rise to new or improved polymer properties, such as, crystallization, molecular dynamics and other properties that have attracted the attention of the polymer researcher community [9–15].

The "in-situ" polymerization of a monomer in the AAO template (nanoreactor) can give rise to the direct production of versatile polymer nanostructures and will avoid the polymer infiltration process. Nevertheless, very little work on the direct polymerization of monomers in reduced spaces of porous aluminum oxide templates has been carried out, since the initial work of Martin et al., about the synthesis of conductive polymer nanostructures [2], even if the number of works studying polymer confinement effects in the last few years has increased a lot. In this sense, it is worth mentioning the polymerizations works of methyl methacrylates (MMA) and other vinyl monomers in nanopores of different nature. Pallikari-Viras et al. [16,17] carried out the polymerization of MMA in silica nanopores and the presence of monomer and polymer in the nanopores followed by Raman Spectroscopy. These authors and Kalogeras et al. [18] have shown that the PMMA molecular weight

* Corresponding author.
E-mail address: cmijangos@ictp.csic.es (C. Mijangos).

0032-3861/$ – see front matter © 2013 Elsevier Ltd. All rights reserved.
http://dx.doi.org/10.1016/j.polymer.2013.10.045

increases during the polymerization in nanopores and the corresponding T_g values and nitrogen absorption is a function of the silica template properties. In addition, in the studies of the reactivity, molecular weight and stereostructure, Uemura and coworkers [19] demonstrated that radical polymerization of vinyl monomers in porous coordination polymers depends on nanochannel size. Very recently, Begum et al. [20] have studied the modeling of MMA free radical polymerization in nanopores finding that the confinement accelerates the reaction rate as a function of borosilicate nanopores size. This author also studied the influence of hydrophilic/hydrophobic character of nanopore in different polymerization parameters [21,22]. Experimental studies about polymerization of MMA in confinement have been made through ATRP and the results interpreted as a function of the molecular weights obtained [23]. In addition, J W Back and coworkers studied the fabrication of conducting PEDOT nanotubes by vapor deposition polymerization using AAO templates [24], Nair et al. reported the Ziegler–Natta polymerization of ethylene inside nanochannels of AAO template [25], functional acidic pyrrole containing oxidizable monomers have been template-polymerized using a hard AAO template in liquid phase polymerization (LPP) conditions [26] and, finally, polybenzyl glutamate has been surface grafted within nanoporous AAO templates and optically characterized [27]. However, in these papers the kinetics of the vinyl polymerization in AAO templates or the characterization of the obtained polymers has not been studied.

As has been extensively reported, to prepare polymer nanostructures by using AAO templates, powdered or film polymer must be infiltrated into the nanocavities at high temperature for a relative long time, from hours to days. Over such time periods degradation of the polymer chain might occur. So, another advantage of the one-step in-situ fabrication of polymer nanostructures in the AAO nanocavities is that degradation problems will be overcome.

The objective of this work is to study the "in-situ" polymerization of a vinyl monomer in the reduced spaces of AAO nanocavities, both to prepare polymer nanostructures and to study the polymerization kinetics under confinement. A second objective is the subsequent characterization of the nanostructured and bulk polymer in order to establish the influence of confinement on the properties of the polymer synthesized into AAO and in bulk.

Following the relatively large body of experimental work done in our laboratory on the preparation and characterization of a wide range of different polymer and polymer based nanostructures of tailored dimensions by polymer infiltration methods [4,10,13], we have set up a methodology to use AAO nanocavities as a nanoreactor by carrying out the polymerization of vinyl monomers, with styrene as the example. For that, SEM morphological studies have been conducted to establish the final structure of the obtained polymer nanostructures. Raman studies have been performed to ascertain the presence of polymer and monomer through the AAO cavities in order to determine monomer conversion. SEC experiments were carried out to evaluate average molecular weights and the polydispersity index of polymer obtained in confinement and in the bulk. NMR measurements helped to determine the effect of nanoreactor in the stereochemistry of PS obtained. TGA, NMR and DSC studies have been performed to compare nanostructured and bulk PS.

2. Experimental section

Monomer and initiator. Styrene monomer (99%) was purchased from Aldrich. Inhibitor free styrene was obtained by washing the monomer with aqueous NaOH solution (10 wt%) and water until neutralization. Subsequently, dried over anhydrous sodium sulphate and distilled under reduced pressure before use. The initiator, 2,2′-azobis-(isobutyronitrile) (AIBN) purchased from Aldrich was purified by recrystallization from methanol before use.

Synthesis of AAO templates. AAO templates have been prepared via a two-step electrochemical anodization process, from around 12 cm^2 aluminum plates, in oxalic acid at a controlled temperature of $T = 2–3$ °C, as described elsewhere [10,28,29]. The dimensions of AAO templates obtained from SEM are 39 nm of pore diameter and 100 μm of pore length (shown in the results section).

2.1. Polymerization reaction

Polymerization of styrene in AAO nanocavities. The polymerization reaction of styrene was carried out in AAO template pores by the so called wet method. Simultaneously styrene was bulk polymerized under the same conditions. For that, AAO templates were previously kept 150 °C in vacuum for 3 h, then were introduced in suitably sized vessels and a solution of AIBN in styrene (0.47% w/v) was added and maintained for 1 h at room temperature and under nitrogen to let the monomer seep into the nanocavities. The AAO templates, containing the infiltrated styrene were placed in an oven at 70 °C under nitrogen (see Scheme 1). At this temperature polymerization of styrene is initiated thermally and carried out inside the templates (nanoreactor) for a set of different times. Simultaneously, bulk polymerization was carried out under the same conditions. After the various different times, the AAO template was drained and introduced into methanol to stop the reaction. After the contact with methanol, the template was placed in vacuum for 3 h and stored in a freezer at −18 °C. n-PS_x is a polystyrene obtained in AAO nanocavities at x hours.

In order to obtain the %conversion of polymerization, the samples in the AAO cavities were removed by successive extraction processes with chloroform with the assistance of ultrasound. This process was repeated until the weight of the dry template was constant and equal to its initial weight. After that, the polymer was precipitated with cold methanol and the %conversion was calculated using the equations (1) and (2):

$$\%\mathrm{Conv} = \frac{W_{\mathrm{n-PS}}}{W_{\mathrm{n-PS}} + W_{\mathrm{n-St}}} \quad (1)$$

$$W_{\mathrm{n-PS}} + W_{\mathrm{n-St}} = W_{\mathrm{AAO+sample}} - W_{\mathrm{AAO}} \quad (2)$$

In equations (1) and (2), $W_{\mathrm{n\text{-}PS}}$ corresponds to n-PS removed from the template by dissolution in chloroform, $W_{\mathrm{n\text{-}PS}} + W_{\mathrm{n\text{-}St}}$ corresponds to PS + St present in the template before extracting with chloroform and was calculated as the difference in weights of the template before (W_{AAO}) and after (W_{AAO} + sample) the extraction procedure.

Polymerizations of styrene in bulk. The bulk polymerization of styrene was carried out in the same conditions as for the polymerization in confinement, in vials of 10 cc containing 3 ml of

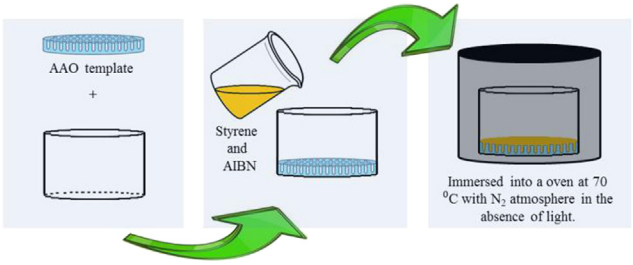

Scheme 1. Experimental methodology used for radical polymerization of styrene in AAO nanocavities.

styrene and AIBN (0.47% w/v). The vials were introduced in an oven at 70 °C under nitrogen and the monomer was allowed to polymerize for the same set of times as those of the polymerization reaction in the nanoreactors. Reactions were quenched by contact with cold methanol and the resulting polystyrene was purified by dissolving it in chloroform and precipitation in cold methanol.

2.2. Structural and chemical characterization

Scanning electron microscopy. Selected samples of polymers obtained in the AAO nanocavities were morphologically characterized by scanning electron microscopy (SEM) (Philips XL-30 ESEM). In order to perform this analysis, the aluminum substrate was eliminated by treatment in a mixture of HCl, $CuCl_2$, and H_2O and, subsequently, the AAO membrane was dissolved in 5% wt H_3PO_4. The polymer being not hydrosoluble could be filtered from the above solution and finally dried for SEM analysis following a procedure described elsewhere [4], (Supporting information).

Confocal Raman microscopy. Selected polystyrene samples confined in the AAO nanocavities were chemically characterized by Raman Spectroscopy, Renishaw InVia Raman Microscope. The Raman scattering was excited with a 785 nm near-infrared diode laser. A 100×, NA090 objective lens was used, giving a laser spot diameter of ~1 μm. With this objective the sampling depth is estimated to be around 4–5 μm (half-width of the confocal depth profile for a silicon wafer) and the lateral resolution is estimated at about 1 μm with the system operated in the confocal mode. The methodology has been described by Maiz et al. [12].

The Raman scattered radiation was focused through a pinhole aperture for confocal geometry and then sent onto the entrance slit (set at an aperture of 50 μm) of a spectrometer (TRIAX 180, Jobin-Yvon). In such a way, the measured lateral and axial resolutions were ~0.52 and ~1.55 μm, respectively. Data acquisition covered the spectral range 3200–100 cm^{-1} with a spectral resolution of 4 cm^{-1} with each exposure of the CCD detector. Depth profiles were obtained by focusing the microscope stepwise, at 10 μm intervals, through the AAO template.

The measurements were carried out for an aliquot of template, that is, polystyrene, alumina and aluminum. Previously, any trace of the supernatant PS polymerized in the template surface was scraped off with the aid of sharp blades (Supporting information).

Size exclusion chromatography. The average molecular weight and the molecular weight distribution of bulk and nanoreactor polymerized PS were determined by SEC in an LKB-2249 instrument at 25 °C. A series of four μ-styragel columns (10^5, 10^4, 10^3,100 Å pore size) were used with chloroform as an eluent. The polymer concentration was 4–5 mg/mL, and the flow rate was 0.5 mL/min. Mass chromatograms of the polymers were detected by a Shimadzu (SPD-10A) UV/VIS detector at 254 nm (for the phenyl group). Polystyrene standards supplied by Polymer Laboratories and Polysciences were used for calibration. The nanoreactor polymerized PS samples were prepared using aluminum disks of 3 cm in diameter and extracted by dissolution (Supporting information).

Nuclear magnetic resonance. The ^1H NMR and ^{13}C NMR spectra of the polystyrene were recorded with a Varian Mercury Plus Spectrometer, 400 MHz. Chloroform-d_1 was used as a solvent. The typical spectral conditions were as follows: spectral width 3201 Hz, acquisition time 4.09 s and 8–16 scans per spectrum. The digital resolution was 0.39 Hz per point. Tetramethylsilane (TMS) was used as the internal standard and the polymer concentration was 6.0 wt% at 40 °C. The samples were prepared using the n-PS extracted by dissolution (Supporting information).

2.3. Thermal characterization

Thermogravimetric analysis. Polystyrenes synthesized either in the AAO nanocavities or in bulk were characterized by Thermogravimetric analysis (TGA Q500-TA Instruments) under nitrogen atmosphere, gas purge at 90 mL/min, and ramp from room temperature to 900 °C. As in Raman spectroscopy, for the polymer synthesized in the AAO nanocavities, the measurements were carried out for the polymer in the template, that is, polymer, alumina and aluminum (Supporting information).

Differential scanning calorimetry. Polystyrene synthesized either in the nanocavities or in bulk was characterized by Differential Scanning Calorimetry (DSC 8500 with HyperDSC-Perkin Elmer) under a nitrogen atmosphere, using processes of heating and cooling of 20 °C/min from room temperature to 230 °C. In this technique it was necessary to remove the aluminum of the AAO nanocavities (Supporting information).

3. Results and discussions

3.1. Synthesis of AAO template

The synthesized AAO templates have been morphologically characterized by scanning electronic microscopy. The study through this technique allows the examination of both the surface and the length of the AAO templates. Fig. 1 shows SEM micrographs at different positions: (a) bird-eye view of AAO template; (b) 3D image of AAO template and (c) 3D lateral view of AAO nanocavities. From these pictures it is observed that the dimensions of the pore nanocavities are very homogeneous of around 35–40 nm of diameter. From Fig. 1c is observed that the length of the nanocavities is 103 μm. We can conclude that the nanoporosity of templates is highly regular in size and order, in other words, the same dimensions of diameter and length are maintained all along the length of the nanocavities. Taking into account the dimensions of each nanocavity and that it is a watertight compartment, each AAO nanocavity can be therefore considered as a nanoreactor.

3.2. Polystyrene synthesis in AAO nanocavities

In this work, the styrene has been selected as an example of vinyl monomer because i) the polymerization of styrene in the AAO nanotemplates has never been reported in the literature, ii) in order to compare the results, the bulk polymerization of this monomer has been widely reported, and iii) because the results obtained could be of great interest, among others, for the direct copolymerization of styrene and tautomeric acrylic monomers in AAO templates. These copolymers are very promising biomaterials to be used as scaffolds for cell growth [13], although some of them are difficult to infiltrate in AAO templates from the melt state.

The polymerization of styrene inside the nanocavities has been carried out as described in the experimental part. Experiments were conducted at different times, from 2 to 50 h, n-PS_x being a polystyrene obtained at x hours in the nanoreactor (n). In parallel, bulk polymerizations were carried out in the same experimental conditions, b-PS_x is a polystyrene obtained at x hours in the bulk conditions (b).

The evidence that the synthesis of polystyrene had been achieved was obtained by scanning electron microscopy (SEM). The morphological study also allowed us to demonstrate that polystyrene nanostructures had been obtained. Fig. 2 shows nanofibers obtained by radical polymerization of styrene in the AAO nanocavities at two different polymerization times. Fig. 2a and b corresponding to n-PS_6, while 2c and d to n-PS_{30}, at different magnifications. These figures show that, firstly the nanofibers have

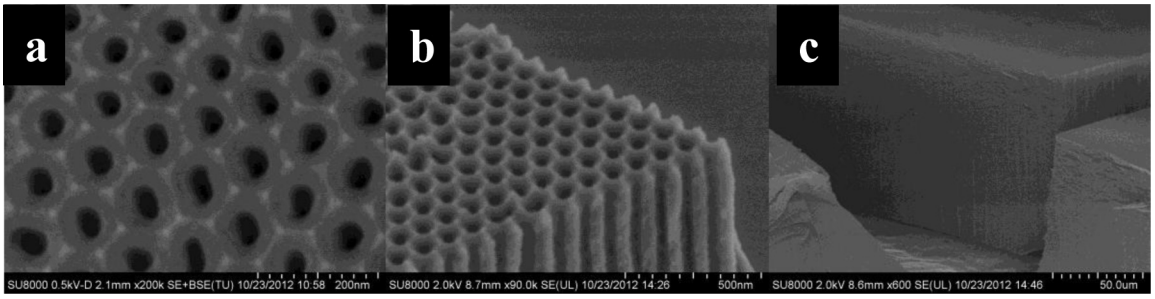

Fig. 1. SEM micrographs of surfaces of prepared AAO templates: (a) top view, (b) 3D image of AAO template and (c) 3D lateral view illustrating AAO longitudinal nanocavities of AAO.

been obtained and therefore polymerization has occurred and, secondly the polymer nanofibers reproduce the dimension of nanocavities. So, a direct fabrication of polystyrene nanofibers of around 35 nm in diameter has been obtained using the discontinuous AAO device for the styrene polymerization reaction. The observed micrographs for both nanostructures are very similar, therefore it cannot be deduced whether monomer remains inside the nanofibers or, in other words, the degree of conversion cannot be deduced.

In order to estimate the monomer conversion at different times of polymerization a confocal Raman microscopy (CRM) study was undertaken to monitor the styrene monomer inside the AAO nanocavities, from the surface up to 60 μm of deepness. CRM spectroscopy method enables us to chemically analyze a polymer or copolymer along the AAO nanocavity by identifying specific bands of compounds through confocal methodology [12]. Fig. 3a shows the Raman spectra of St and PS. The signal at ~1630 cm^{-1} corresponds to the C=C stretching band, which is present only in the monomer; while the signal at ~1600 cm^{-1} corresponds to C=C aromatic stretching band, present in both monomer and polymer, and thus represents 100% of the sample. Therefore, the peak at 1630 cm^{-1} allows us to identify and quantify the amount of monomer at different depths of the nanocavity.

As an example, Fig. 3b shows an enlargement of normalized Raman spectrum (between 1550 and 1650 cm^{-1}) for n-PS_3 sample as a function of the depth of the nanocavities. It is possible to see that the Raman band at 1630 cm^{-1} shows a small change in its intensity along the depth of the nanopores (the intensity of the peak at 60 microns is smaller than the intensity at 0 microns), indicating a gradient in the monomer conversion along the nanopores. This behavior suggests that the monomer polymerizes more rapidly from below to above the pore, which could be due to establishing a decreasing temperature gradient in this direction (from the bottom up) because the nanomold lower surface is in contact with the inner surface (floor) of the heating furnace, while the top of nanopore senses the inert atmosphere that surrounds it.

The I_{St}/I_{Ar} relationship allows to quantify the presence of styrene monomer along the nanocavity. I_{St} and I_{Ar} correspond to the signal intensity at ~1630 cm^{-1} and at ~1600 cm^{-1}, respectively. Table 1 collects the average values of I_{St}/I_{Ar} throughout the nanocavities (from 0 to 60 μm in Fig. 3b) for the different n-PS samples at a given time, *x*, not shown here (Supporting information). In order to determine the monomer conversion, a calibration curve using different monomer and polymer composition was made (Supporting information). The linear regression obtained allowed us to estimate the monomer conversions whose values are shown

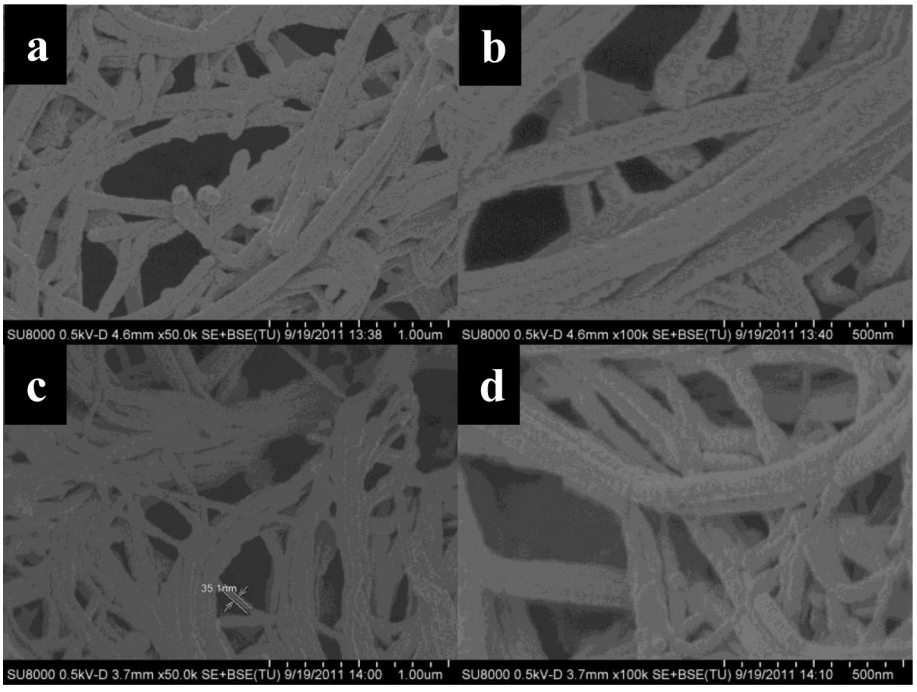

Fig. 2. Nanofibers obtained by radical polymerization of styrene into AAO template; (a) and (b) corresponding to n-PS_6 while (c) and (d) to n-PS_{30}.

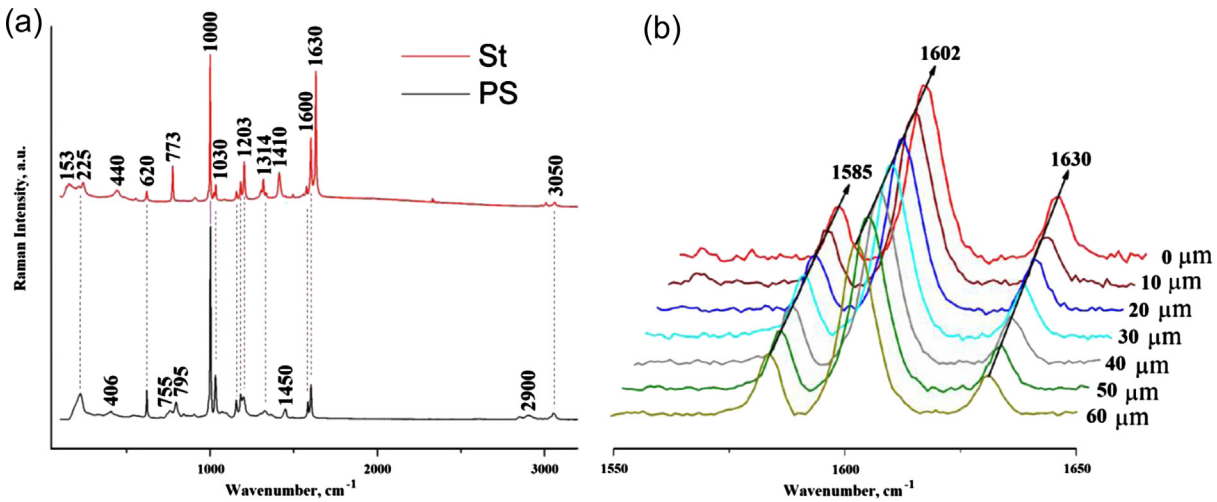

Fig. 3. Raman spectra of (a) St and PS with assignation of differences between both spectra, (b) change of the Raman spectrum (between 1550 and 1650 cm^{-1}) as a function of depth of nanocavities for n-PS_3.

in Table 1. In addition, the monomer conversions obtained by polymer extraction of the template and the corresponding values for the bulk polymerization (determined by gravimetry) are included for comparison, see experimental part for details.

From these results it can be seen that the PS %conversions under confinement evaluated by Raman and gravimetric measurement are similar and higher than the PS %conversion under bulk polymerization conditions. Moreover, from the %conversion data it is possible to evaluate the rate of polymerization (R_p), using the following equation:

$$R_p = \frac{d.\%\mathrm{Conv}.10}{t.\mathrm{Mo}} \quad (3)$$

where,

d = monomer density (g/cm^3)
t = reaction time in s
Mo = molecular weight of the monomer

In Fig. 4, the plot of R_p versus time shows a sharp increase up to 2.5 h reaction time followed by a slight decrease. Under the same polymerization conditions, the bulk reaction exhibits a R_p almost three time lower than the reaction rate carried out under confinement.

The observed behaviors suggest a catalytic effect of the AAO template on the rate of polymerization and provides good evidence of the confinement effect. Although for free radical polymerization confined to the nanoscale little kinetic data are available in the literature, our results are in agreement with those found by other researchers who studied the effect of confinement on the methyl methacrylate free radical polymerization in pore glasses of different sizes and polarity pore surface [20,30]. These authors attribute the observed kinetics change to a decrease in the diffusivity of active chains upon confinement, which is more strongly influenced than the propagation reaction, governed by diffusion of the monomer.

Table 1
Conversion degree obtained for selected n-PS and b-PS by CRM and gravimetric (Grav).

n-PS_x (x, h)	Average I_{St}/I_{Ar}CRM	Conv. n-PS (CRM) (%)	Conv. n-PS (Grav.) (%)	Conv. b-PS (Grav.) (%)
2	0.8 ± 0.1	46.2	–	13
3	0.72 ± 0.04	53.8	59.7	23
6	0.65 ± 0.05	78.9	71.6	47
24	0.58 ± 0.05	86.7	84.4	75

3.3. Characterization of the polymers

In order to characterize the molecular weight and polydispersity of the polymer nanostructures and eventually to study if the polymerization process in confinement in the nanoreactor is the same as in the bulk, the variation of molecular weight and polydispersity, as a function of time, has been studied and the results compared to those of the bulk by means of size exclusion chromatography (SEC). Fig. 5(a and b) presents the normalized chromatograms for b-PS and n-PS, respectively. From a general view, differences between both kinds of polymers are easily appreciated. SEC chromatograms of n-PSs are monomodal at all reactions times.

The chromatographic profile of b-PS becomes bimodal, as a result of a new second macromolecule population as time increases. This behavior can be attributed to the relatively high viscosity attained at high conversion (>40%), which retards the termination and chain transfer reactions, as was proved for a number of systems [31]. This effect leads to a higher molecular

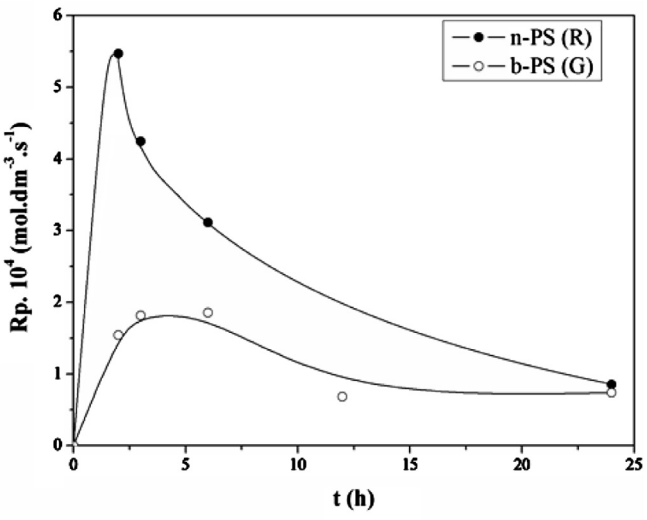

Fig. 4. Rate of polymerization of St under confinement by Raman (R) determination and bulk by gravimetric (G) determination. Reaction conditions: [AIBN] = 0.47% w/v; T = 70 °C.

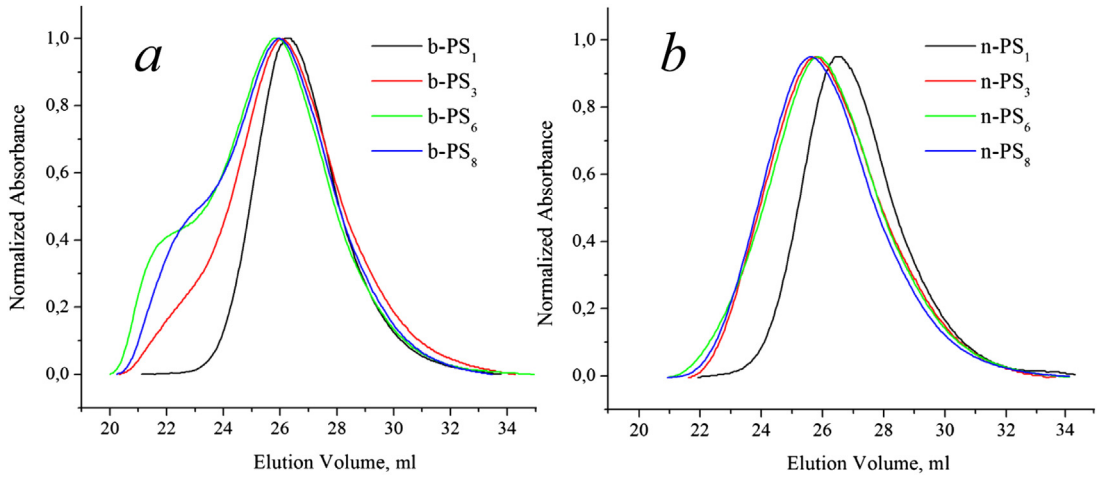

Fig. 5. Chromatographic profile for (a) bulk and (b) nanopolymerization.

weight contribution of the bimodal distribution as time increases, because at the highest conversion, the termination rate is always diffusion-controlled. Fig. 6 shows the weight average molecular weight (M_w) and polydispersity index (PDI) of the obtained polymers as a function of the percentage of conversion. It can be seen that up to 50% conversion no significant differences in M_w or PDI in both polymerization processes occurs, which means that the growth radical termination mechanisms is the same in both cases. At high conversion (>65%), it is observed that M_w and PDI values are higher for bulk polymerization than nanopolymerization and that for the former case the increase is more pronounced as the reaction conversion progresses. This behavior could be attributed to the better control of the temperature inside of the nanomold, in comparison to the bulk polymerization, where the heat transfer will occur in a very much higher volume.

The PDI values close to 2 suggest, based in theoretical predictions, that disproportion and/or chain transfer mechanisms are the predominant termination modes [32]. Therefore, even at high reaction conversions the distribution is monomodal with good control of M_w. If we compare our results with the bibliographic results, some differences are present. Studies of other researchers have showed an increment of M_w values in confinement [19–22], in particular, inside silica and borosilicate templates, MMA shows an increment of the M_w value. In our case, we attribute the observed differences to the nature of monomer and nanoreactor. The polymerization was carried out using a non-polar monomer (styrene) and AAO templates, these differences suggest that these parameters are crucial on the obtained molecular weight.

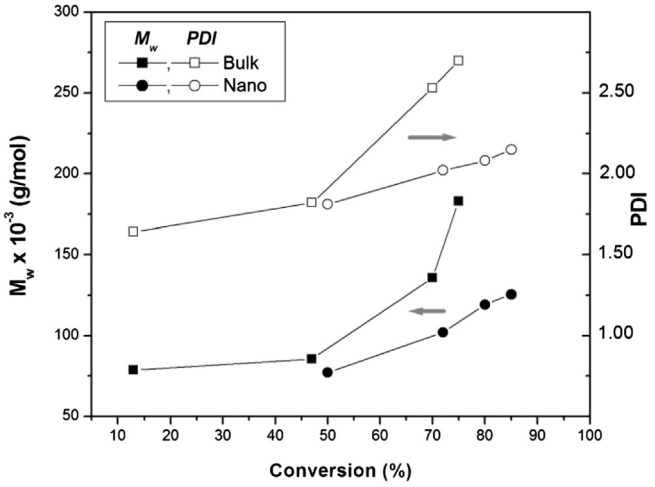

Fig. 6. M_w and PDI as a function of conversion, n-PS (●, ○) and b-PS(■, □). Weight average molecular weight (M_w) and polydispersity index (PDI) determined by SEC.

In this work, a preliminary NMR study has been made in order to check any possible effect of nanoconfinement on the stereochemical structure of obtained polystyrene. For this purpose, ^{13}C NMR spectra of n-PS_{24} and b-PS_{24} have been compared. Fig. 7a presents ^{1}H NMR spectrum of n-PS_{24}. The signals between 1.2 and 2.5 ppm correspond to methylene and methyne groups of the main chain, whereas the signals between 6.2 and 7.5 ppm include all aromatic protons. From the ^{13}C NMR spectrum (Fig. 7b), the following C assignations are obtained: δ_C (300 MHz; $CDCl_3$; Me_4Si) 145.72 (aromatic ipso-carbon), 128.22 and 125.85 (aromatic signals), 44.50 (>CH–Ar), 40.73 (–CH_2–).

^{13}C NMR signals of the phenyl ipso-carbon and the methylene carbons are used for the determination of the tacticity of polystyrene [33]. More precisely, the determination of ipso-carbon signals through pentads analysis, presents some advantages as mentioned by other authors [34]. In Fig. 7c, it is possible to observe the differences between the deconvolutional analysis ^{13}C NMR for n-PS_{24} and b-PS_{24} in the ipso-carbon zone. According to Bernoullian statistics, for a 100% syndiotactic PS in the pentads analysis, four distinguishable signals appear in the phenyl ipso carbon, in intensity ratios, from left to right, of 1.0:1.0:5.9:1.0 [35]. It is clear that if syndiotacticity decreases, the relationship will not be maintained. For n-PS (Fig. 7c) the values found for this relation are 1.0:1.7:3.1:1.0 while for b-PS (Fig. 7c) are 1.0:1.07:1.38:1.42. These results show that n-PS with a value of 3.1 for the syndiotactic signal has a higher degree of syndiotacticity than b-PS, 1.38. An interesting study about the tacticity of polymers obtained by polymerization in porous coordination polymers of vinyl monomers [19] has demonstrated an effect of pore size in the isotactic degree. Monomers with polar groups (carbonyl groups) have showed this effect. In our case, we cannot attribute this difference to any particular confinement effect but why not speculate if difference in the diffusion of growing chains in confinement in regard to bulk and/or nanocavities wall obstruction, could favor a kind of regiorigidity of the chain and would allow a rather stereoregular growing? Be as it may, this preliminary study suggests an interesting way of obtaining the PS of higher syndiotacticity PS using discontinuous AAO devices in comparison to bulk.

Thermogravimetric analysis of selected samples has been carried out in order to compare the thermal stability of the obtained

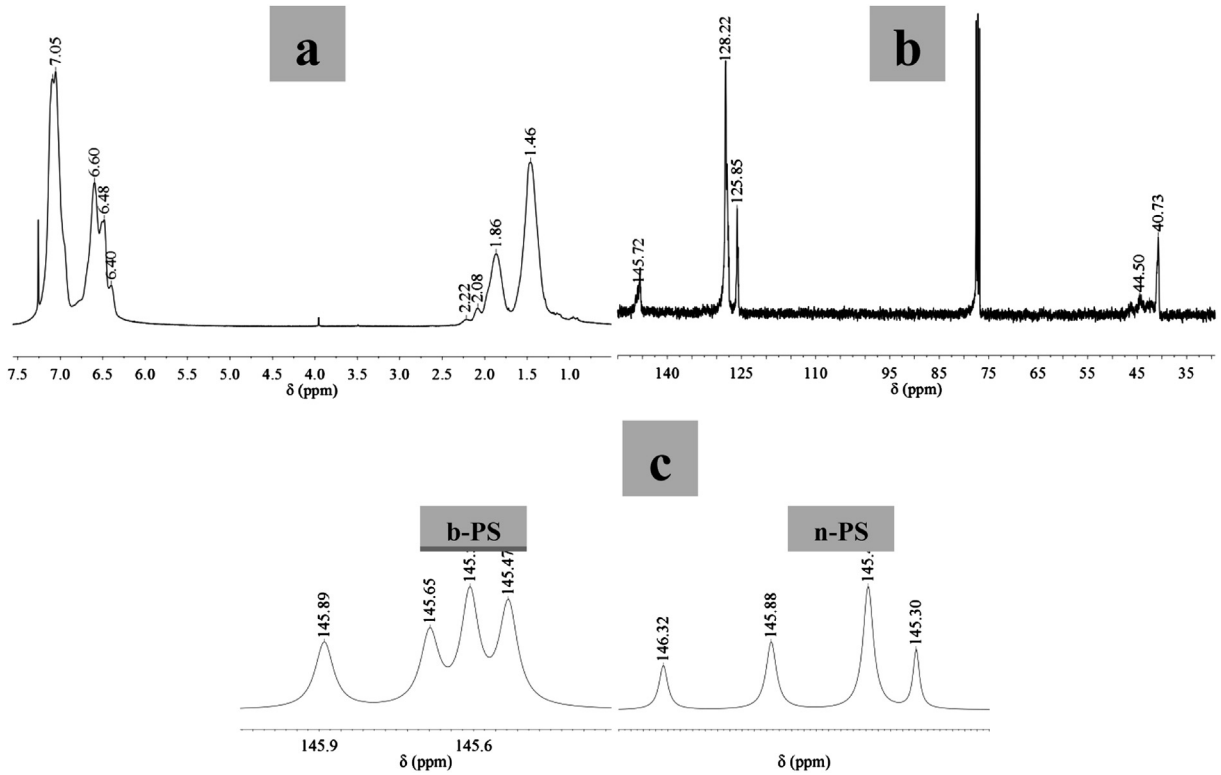

Fig. 7. NMR spectra for PS_{24} (a) ^{1}H NMR, (b) ^{13}C NMR and (c) deconvolutional analysis ^{13}C NMR for b-PS_{24} and n-PS_{24} in the ipso-carbon zone.

polystyrenes, n-PS and b-PS. Table 2 shows the tabulated values of peak maximum temperature in derivate weight loss and onset point in the TGA profile.

From these results it is important to note that n-PSs are considerably more thermally stable than the respective b-PSs. Moreover, the difference in peak maximum and onset point temperature values for n-PS_6 and b-PS_6, 39 °C and 53 °C respectively, greatly exceeds the differences obtained for many polymers confined by nanopore infiltration and their counterparts in bulk [36,37].

In addition, degradation curves for n-PS_4 and b-PS_4 are plotted in Fig. 8. For bulk PS the presence of one thermal event is observed while for PS polymerized in the nanocavities, two thermal events are seen, suggesting the influence of other parameters in the degradation of the polymer as, for instance, the syndiotacticity of the polymer. In fact, Chen et al. [38] have studied the tacticity as a factor contributing to the thermal stability of polystyrene and found differences between the thermal degradation depending on the tacticity of PS, syndiotactic PS being thermally more stable than atactic PS. For this reason we suggest if, in our case, the presence of the second thermal event of n-PS could be due to the contribution of a higher syndiotactic degree, assuming that the first event would correspond to the atactic parts and the second event to syndiotactic parts of the polymer, thermally more stable.

Other evidence of the influence of confinement effects in PS polymerization is shown in the preliminary study of the glass transition temperature carried out by DSC. Table 3 shows the T_g values of selected n-PS and their analogous b-PS samples, the first one being higher than the second and therefore evidencing differences between both samples. Although it is not the objective of the present work to go deeper in this study, recent works in literature have shown that confinement increases the T_g values, depending on the nature of the system, suggesting that confinement directly affects the cooperative movements of the polymer chains. For instance, Shin et al. found confinement effects for polystyrene infiltrated in AAO templates and claimed that their results were similar to those of supported ultrathin films [39]. Additionally, in previous work, we have found 2 °C of difference in the T_gs obtained for PS bulk and PS nanostructured obtained by infiltration of PS in AAO of the same dimensions as used in the present work [13]. In the present case, it is possible that a more syndiotactic PS as obtained in confinement could stiffen even more the polymer chains. Therefore, the cooperative movement would be even more limited, giving rise to an increase of the T_g values.

Table 2
TGA analysis for n-PS and b-PS.

Polymer	Peak maximum in deriv. weight (°C)	Onset point (°C)
n-PS_6	454	443
n-PS_{30}	452	440
b-PS_6	415	390
b-PS_{30}	422	398

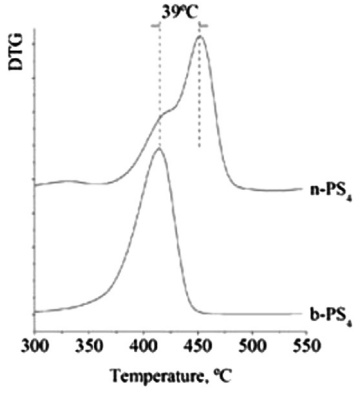

Fig. 8. TGA curves for degradation of n-PS_4 and b-PS_4 represented in the normalized derivate of the TGA curves (DTG).

Table 3
DSC studies for polystyrenes synthesized.

Polymer	T_g in onset point (°C)	T_g half Cp extrapolated (°C)
b-PS_{20}	100	102
b-PS_{24}	102	105
n-PS_{20}	110	110
n-PS_{24}	111	110

In summary, this work shows that porous anodic aluminum oxide (AAO) nanocavities can be used as nanoreactors both to prepare polymer nanostructures and to study the radical polymerization kinetics of a vinyl monomer in confinement. PS polymerized in confinement in porous aluminum oxide templates presents important chemical/physical differences compared with PS polymerized in bulk: the weight average molecular weight and the polydispersity index of polymers from confinement are lower than those from bulk; differences in the stereostructure of both kind of samples are observed; nanostructured polymers are more thermally stable than bulk polymers and differences in T_g temperature between nanostructured and bulk PS are noticeable.

4. Conclusions

In this work, porous anodic aluminum oxide (AAO) templates of 35 nm diameter have been obtained and used as nanoreactors to study the radical polymerization of styrene (St) in confinement. The polymerization kinetics of styrene in porous AAO nanocavities (n-PS) has been studied as a function of time and compared to the polymerization in bulk (b-PS). SEM morphological studies have allowed the establishment of the final structures of the polymers nanoforms obtained and confocal Raman spectroscopy has revealed that polymer has been obtained through the whole length of the AAO cavities. This experiment has allowed us to estimate the reaction conversion. SEC experiments show monomodal chromatograms for n-PSs at all reactions times, while for b-PS the chromatographic profiles indicate bimodal behavior from 6 h. Weight average molecular weights and the polydispersity index of polymer from confinement are lower than those from bulk polymerization. TGA studies have allowed us to demonstrate that nanostructured polymers are thermally more stable than bulk polymers. Finally DSC analysis has also shown differences in T_g between nanostructured and bulk PS, the T_g of n-PS being higher than that of b-PS. The observed differences could be attributed to differences in the tacticity degree of both samples.

Although a deeper study about the effects of nanoconfinement on the properties of PS obtained in the AAO nanotemplates is needed, the methodology and results shown in this work demonstrate that the polymerization reaction in AAO nanocavities is a complementary way to obtain tailored thermoplastic polymer nanostructures, and the only way to obtain thermoset polymer nanostructures.

Acknowledgments

J.M. Giussi would like to thank to La Plata National University and CONICET from Argentina. I. Blaszczyk-Lezak acknowledges CSIC for the JAE postdoctoral contract. Financial support from the MINECO, MAT2011-24797 and PRI-PIBAR-2011-1400 is also acknowledged.

Appendix A. Supplementary data

Supplementary data related to this article can be found at http://dx.doi.org/10.1016/j.polymer.2013.10.045.

References

[1] Martin CR. Science 1994;266:1961.
[2] Sapp SA, Lakshmi BB, Martin CR. Adv Mater 1999;11:402.
[3] Grimm S, Lange A, Enke D, Steinhart M. J Mater Chem 2012;22:9490.
[4] Martín J, Maiz J, Sacristan J, Mijangos C. Polymer 2012;53:1149.
[5] Grimm S, Martín J, Rodriguez G, Fernández-Gutierrez M, Mathwig K, Wehrspohn RB, et al. J Mater Chem 2010;20:3171.
[6] Martín J, Nogales A, Martín-González M. Macromolecules 2013;46:1477–83.
[7] Martín J, Martín-González M. Nanoscale 2012;4:5608.
[8] Azzaroni O, Aaron Lau KH. Soft Matter 2011;7:8709.
[9] Sergei A, Zhao W, Miranda D, Russell TP. Nano Lett 2013;13:577.
[10] Martín J, Mijangos C. Langmuir 2009;25:1181.
[11] Guan Y, Liu G, Gao P, Li L, Ding G, Wang D. Macro Lett 2013;2:181.
[12] Maiz J, Sacristan J, Mijangos C. Chem Phys Lett 2010;484:290.
[13] Giussi JM, Blaszczyk-Lezak I, Allegretti PE, Cortizo MS, Mijangos C. Polymer 2013;54:5050.
[14] Maiz J, Schäfer H, Rengarajn GT, Hartmann-Azanza B, Eickmeir H, Haase M, et al. Macromolecules 2013;46:403.
[15] Suzuki Y, Duran H, Steinhart M, Butt H-J, Floudas G. Soft Matter 2013;9:2621.
[16] Li X, King TA, Pallikari-Viras F. J Non-Cryst Sol 1994;170:243.
[17] Pallikari-Viras F, Li X, King TA. J Sol-Gel Sci Technol 1996;7:203.
[18] Kalogeras IM, Neagu ER. Eur Phys J E 2004;14:193.
[19] Uemura T, Ono Y, Kitagawa K, Kitagawa S. Macromolecules 2008;41:87.
[20] Begum F, Simon SL. Polymer 2011;52:1539.
[21] Begum F, Zhao H, Simon SL. Polymer 2012;53:3238.
[22] Begum F, Zhao H, Simon SL. Polymer 2012;53:3261.
[23] Gorman CB, Petrie RJ, Genzer J. Macromolecules 2008;41:4856.
[24] Back JW, Lee S, Hwang CR, Chi CS, Kim JY. Macromol Res 2011;19:33.
[25] Nair S, Naredi P, Kim SH. J Phys Chem B 2005;109:12491.
[26] Esman N, Lellouche J-P. Polym Chem 2010;1:158.
[27] Lau KHA, Duran H, Knoll W. J Phys Chem 2009;113:3179.
[28] Masuda H, Fukuda K. Science 1995;268:1466–8.
[29] Vázquez M, Pirota K, Hernández-Vélez M, Prida VM, Navas D, Sanz R, et al. J Appl Phys 2004;95:6642.
[30] Zhao H, Simon SL. Polymer 2011;52:4093.
[31] Arcos-Casarrubias JA, Olayo R, Noriega Bernechea J. J Polym Sci Part A Polym Chem 2005;43:178.
[32] Odian G. Principles of polymerization. New York: McGraw-Hill; 2004.
[33] Bovey FA. NMR of polymer. San Diego: Academic Press; 1996.
[34] Feil F, Harder S. Macromolecules 2003;36:3446.
[35] Ishihara N, Seimiya T, Kuramoto M, Uoi M. Macromolecules;186:(9):2464.
[36] Blaszczyk-Lezak I, Maiz J, Sacristan J, Mijangos C. Ind Eng Chem Res 2011;50:10883.
[37] Li J-J, Song G-J, She X-L, Han P, Peng Z, Chen D. Polym J 2006;38:554.
[38] Chen K, Harris K, Vyazovkin S. Macromol Chem Phys 2007;208:2525.
[39] Wu Hui, Wang Wei, Yang Huixian, Su Zhaohui. Macromolecules 2007;6:961.